

HAO-JIE SONG<sup>1,2</sup>  
ZHAO-ZHU ZHANG<sup>1,✉</sup>  
XUE-HU MEN<sup>1,2</sup>

# Superhydrophobic PEEK/PTFE composite coating

<sup>1</sup> State Key Laboratory of Solid Lubrication, Lanzhou Institute of Chemical Physics, Chinese Academy of Sciences, Lanzhou 730000, P.R. China  
<sup>2</sup> Graduate School, Chinese Academy of Sciences, Beijing 100039, P.R. China

Received: 14 September 2007/Accepted: 31 October 2007  
Published online: 19 December 2007 • © Springer-Verlag 2007

**ABSTRACT** A simple and inexpensive method for forming a PEEK/PTFE superhydrophobic surfaces by controlling the topographical microstructures by adjusting the curing temperature has been proposed. The resulting porous surface, with ribbon-like randomly distributed double-scale structure and the lowest surface energy hydrophobic groups ( $-\text{CF}_3$ ) has a water contact angle of  $161^\circ$ .

PACS 06.60.Ei; 81.05.Rm; 81.20.Ev; 82.80.Pv

## 1 Introduction

In recent years, there has been a great deal of research interest in fabricating superhydrophobic surfaces, which have static contact angles of water droplets greater than  $150^\circ$ , because of their importance in fundamental research [1, 2] as well as in practical applications of biomimetic systems, such as preventing the adhesion of snow or rain to antennas and windows [3], producing stain-resistant textiles [4], and wettability switching surfaces [5–7]. The superhydrophobic property is believed to be governed by both the chemical composition of the surface material and the cooperative effect of nanostructures within the micrometer-scale areas (the so-called hierarchical structure). For example, the leaves of the lotus and taro and the wings of the cicada have superhydrophobic surfaces [8–11], and they can undergo self-cleaning by removal of dust and pollutants using rolling water drops; this is usually called the “lotus effect” [5, 9, 10].

Several similar studies have been performed on high technological materials such as nanotubes coated by PTFE [12], high porosity materials, [13] polymer nanofibers or nanopatterned surfaces [14, 15]. These materials are superhydrophobic i.e., have a contact angle superior to  $150^\circ$ , but their elaboration presents some disadvantages such as complicated deposition techniques, multi-step processes and low surface coverage. Recently, some researchers [16, 17] have demonstrated that a bionic polymer surface with superhydrophobicity can be prepared by one-step casting process under an ambient atmosphere. However, the cohe-

sional strength between the polymer coatings and glass substrate was very weak, and easily scraped off. Furthermore, it did not provide long-term stability over a wide pH range, that is, neither for pure water nor for corrosive liquids including acidic, basic and salt. Therefore, the above techniques limit the practical applications of superhydrophobic surfaces. Conventional fluorine polymer hydrophobic coating surface with low surface energy has been used as anti-sticking, anti-fouling and reduction drag and flow noise [18, 19]. However, the ordinary fluorine polymer hydrophobic surfaces have merely the water contact angles of  $110$ – $125^\circ$  without super-hydrophobic, anti-ice and self-cleaning properties.

In the present work, the superhydrophobic surfaces of the PEEK/PTFE composite coating were prepared using conventional simple spray processes on a steel 45 substrate. The coating shows stable superhydrophobicity, even in many corrosive solutions, such as acidic or basic solutions. Compared to the superhydrophobic surface mentioned above, our preparation method is much simpler and easily scalable. Such one-step coatings are highly interesting for applications in the fabrication of microfluidic devices, fluid microchips and microreactors.

## 2 Experimental part

The powder of PTFE (FR002A, average diameter of  $5\ \mu\text{m}$ ) were provided by Shanghai 3F News Materials CO.LTD, China. The  $10\ \mu\text{m}$  PEEK powder used in this study was supplied by Jilin university. Single-component polyurethane was provided by Xinhua Resin Company of Shanghai, and the ash content and the isocyanate content were 50 and 5–8 wt. %, respectively.

The AISI 1045 block was polished with 800 grade waterproof abrasive paper in turn and then cleaned with acetone in an ultrasonic bath for 5 min. To obtain a slurry of PEEK and PTFE, the powder of PEEK and PTFE with a weight ratio of PTFE to PEEK of 3 : 1 was dispersed in the mixed solvent with ultrasonic stirring for 30 min. Then both the PU binder and the suspension with a weight ratio of PTFE to PU of 3 : 1 were carefully mixed by mechanical stirring and ultrasonic treatment. The coatings on Fe blocks were prepared by spraying the coating precursors with 0.2 MPa nitrogen gas and then cured at room temperature, 120, 200, 250 and  $300^\circ\text{C}$  for 2 h,

✉ Fax: +86 931-4968098, E-mail: zzzhang@lzb.ac.cn

respectively. The thickness of the cured coatings was about 10–100  $\mu\text{m}$ .

The topographical microstructures of the PEEK/PTFE composite coating at different curing temperatures were observed by scanning electron microscopy (SEM; JEOL, JSM-5600LV). The chemical state of the elements in the superhydrophobic surface was identified using a multi-functional X-ray photoelectron spectroscopy (XPS) (PHI-5702, Perkin-Elmer, USA). The  $\text{Mg } K_{\alpha}$  line was used as the excitation source. The binding energy 284.6 eV of C1s in hydrocarbon was used as reference. The sessile drop method was used for water contact angle measurements with a CA-A contact angle meter (Kyowa Scientific Company, Ltd.; Japan) at ambient temperature. Water droplets (about 10 mg) were dropped carefully onto the surface. The average WCA value was determined by measuring five different positions of the same sample, and their images were captured with a traditional digital camera (Sony).

### 3 Results and discussion

The shapes of water droplets on PEEK/PTFE composite coating surfaces at different curing temperatures are shown in Fig. 1. Droplets with spherical shapes are floating on the as-prepared surfaces uniformly, with CA values of around 123, 145 and 161°, respectively. The change of the surface microstructures by increasing the curing temperature was responsible for the increase of CA. At higher curing temperatures, the solvent evaporates more quickly, thus increasing the pore formation. Therefore, the inhomogeneity and size of the pores increase with the increase of the curing temperature. Most importantly, water droplets on the surfaces of structure C freely roll off the surface without becoming pinned, even after sitting on the surface for long times. Remarkably, this surface remained superhydrophobic after being immersed in water for at least a week or in a high humidity environment for at least 3 months. In contrast, water droplets on the surfaces of structure A start pinning after sitting on the surface for a couple of minutes, suggesting a transition from the Cassie state to the Wenzel state.

Interestingly, the water CAs are larger than 150° not only for pure water but also corrosive liquids, such as acidic and basic aqueous solutions. Figure 2 shows effect of storage time on the water CAs at different pH values. There is no obvious fluctuation of the water CAs on the resulting surface within experimental error when the pH is 7.0, keeping a constant value of about 161°, indicating that the storage time has little or no effect on the water CAs. However, the water CAs decrease gradually with increasing time when the pH values are 1.0 and 13.0. The CAs of acidic solution changed from about

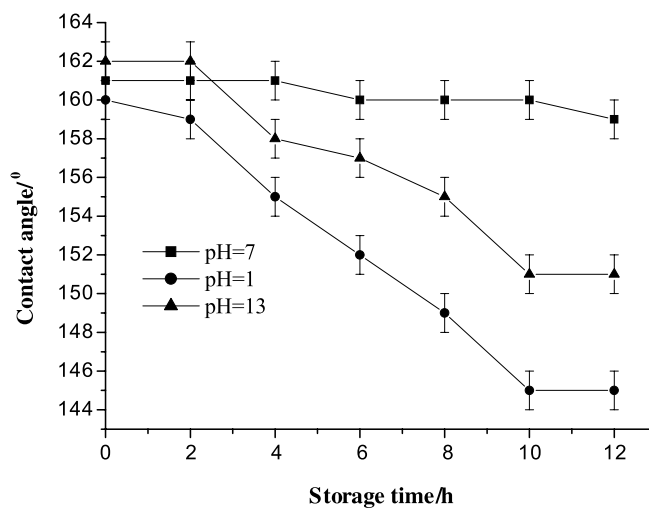


FIGURE 2 Effect of storage time on the contact angle of water at different pH values

160 to 145° when storage time increased from 0 to 12 h, and the CAs of basic aqueous solution changed from about 162 to 151° when storage time increased from 0 to 12 h. These results are very important for the use of iron as engineering materials with superhydrophobic surfaces in the wide pH range of corrosive liquids.

Figure 3 shows the microstructures of the PEEK/PTFE composite coating at different curing temperatures. When the curing temperature was at 25 °C, the surfaces were composed of fine particles of several tens of micrometers (Fig. 3a). More detailed morphology is shown in Fig. 3b. It can be seen that the surfaces were entirely built by the stacking of the particles. The surfaces exhibited surface pores on the order of 1–10  $\mu\text{m}$  and a rough microstructure with pores of about 4  $\mu\text{m}$ . As the curing temperature increased to 200 °C, the surface morphology was similar but with a more regularity in the particle size (Fig. 3c). The enlarged view of the surfaces (Fig. 3d) indicated a honeycomb-like texture with sharp ridges and surface pores as large as 5  $\mu\text{m}$  appeared on the surfaces. Surface roughness increased because of the irregular stacking of the particles and CA raised to  $145 \pm 2^\circ$ . When the curing temperature was further increased to 300 °C, it is interestingly found that ribbon-like randomly distributed structures were formed on the surfaces (Fig. 3e). As shown in Fig. 3f, the surface consisted of fibrous crystals with a large fraction of void space. The surface structures are double-scale (micro and nanostructures) and cover a large surface area, achieving a superhydrophobic surface. These results indicate that the curing temperature also dramatically influences the structures of the PEEK/PTFE composite coating.



FIGURE 1 Optical images of a few water droplets on the surface of the PEEK/PTFE composite coating at different curing temperatures: (a) at 25 °C; (b) at 200 °C; (c) at 300 °C

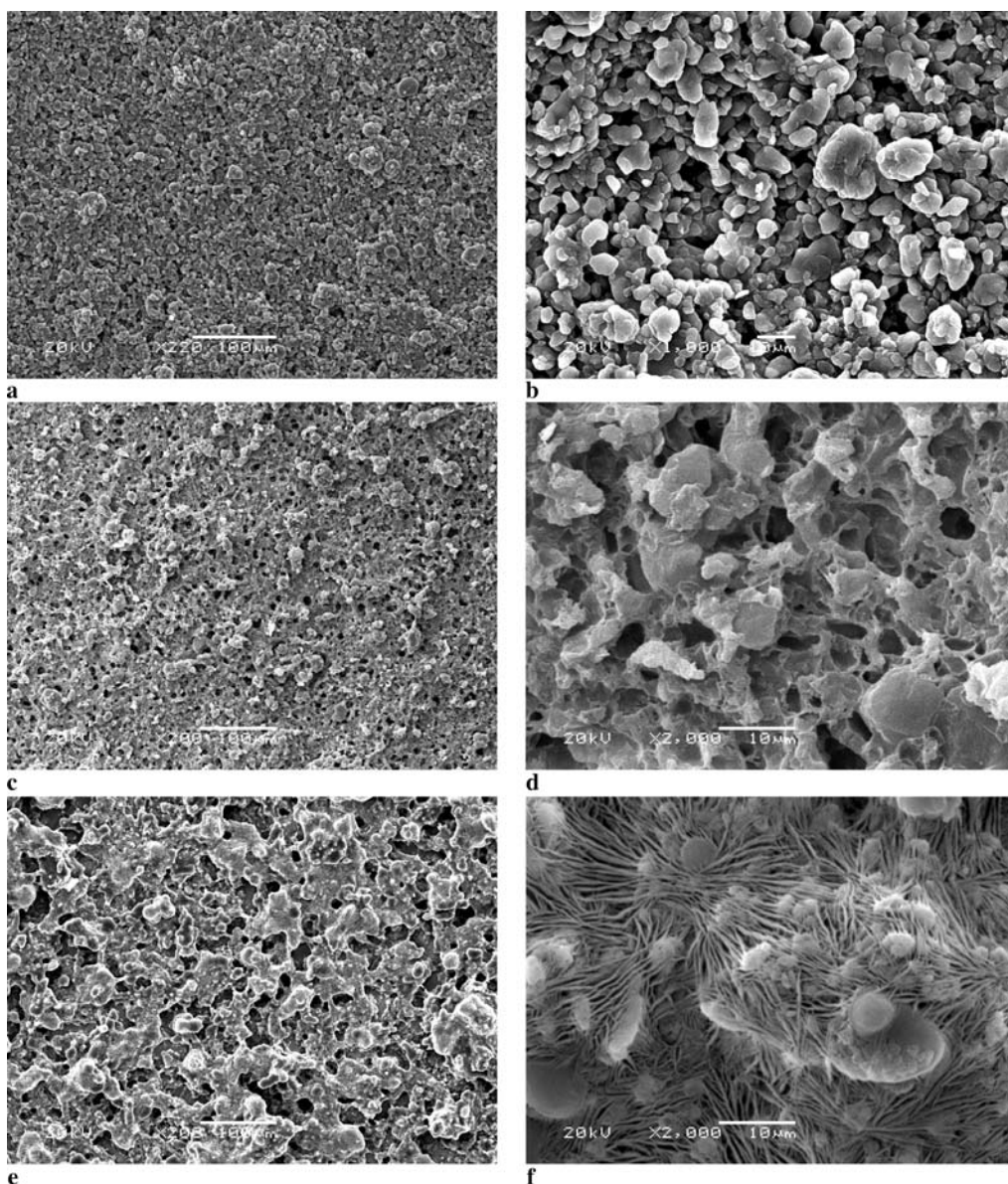


**FIGURE 3** SEM images of the PEEK/PTFE composite coating at different curing temperatures. (a) at room temperature; (b) the high magnification of (a); (c) at 200 °C; (d) the high magnification of (c); (e) at 300 °C; (f) the high magnification of (e)

Accordingly, the influence of surface roughness on water-repellent performance can be suggested by Cassie–Baxter equation between the apparent contact angle  $\theta^*$  observed on a rough surface and the equilibrium contact angle obtained on a smooth surface of the same chemical composition:

$$\cos \theta^* = -1 + \phi_s (\cos \theta + 1),$$

where the surface fraction  $\phi_s$  corresponds to the ratio of the surface of the top of the roughness in contact with the liquid with the apparent surface of the substrate. The value  $h$  relies on the Young's relation,

$$\cos \theta = (\gamma_{SV} - \gamma_{SL}) / \gamma_{LV},$$

where  $\gamma_{SV}$ ,  $\gamma_{SL}$  and  $\gamma_{LV}$  are the interfacial-free energy per unit area of the solid–vapor, solid–liquid, and liquid–vapor interfaces, respectively.

Theoretically, the Cassie–Baxter equation is considered to contribute the effect of roughness on wettability [20, 21].

The model provides a strong deduction for supporting the influence of surface characteristics on contact angle, i.e., surface roughness enhances super hydrophobic behavior. Surface roughness is generally affected by increasing solid ratio since particles are piled up randomly to create a rough surface. Therefore, a spherical water droplet is laid on this composite surface, a patchwork of solid and air. The treated surface in the present work is textured with a nanoscaled hills and valleys that are decorated with fibrous crystals and hydrophobic fluorocarbon material. The hills and valleys ensure that the surface contact area available to water is very low while the hydrophobic fibrous crystals prevent penetration of water into valleys. The net result is that water cannot wet the surface; it forms nearly spherical water droplets, leading to superhydrophobic surfaces.

X-ray photoelectron spectroscopy (XPS) confirmed that the superhydrophobic surface of the PEEK/PTFE composite coating was modified with the curing temperature (Fig. 4). The XPS spectrum of the PEEK/PTFE composite coating

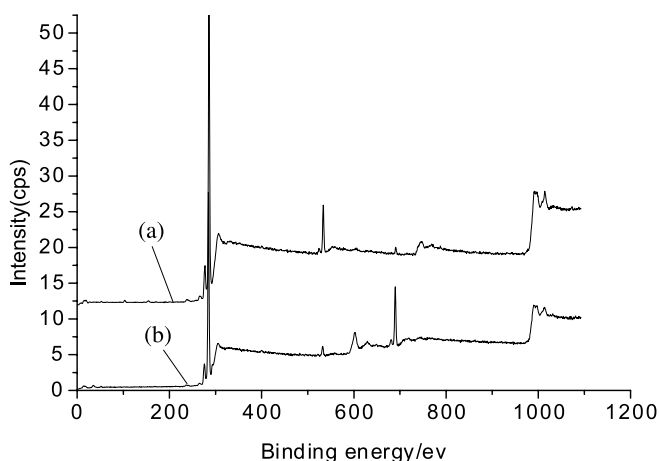


**FIGURE 4** XPS spectra of the PEEK/PTFE composite coating surface at different curing temperatures. (a) At room temperature; (b) at 300 °C

surface at lower curing temperature showed weak detectable fluorine peaks (Fig. 4a), whereas the spectrum at higher curing temperature displayed a strong fluorine peak at 688 eV (Fig. 4b). Owing to the low surface energies, PTFE cannot uniformly disperse in PEEK/PTFE composite coating and is easy to transfer to the surfaces of the composite coating at higher curing temperature. As a result, an increase of curing temperature also can improve the extent of roughness, moreover, causing more proportion of fluoro-binder on the rough surface.

#### 4 Conclusions

In conclusion, our results provided a very easy and economical method for fabricating superhydrophobic polymeric surfaces on steel 45. It is believed that the change of the microstructures, by changing curing temperature, was responsible for the superhydrophobic surface since it had a great effect on the formation of the porous and ribbon-

like randomly distributed structures and the lowest surface energy hydrophobic groups ( $-\text{CF}_3$ ). The super-hydrophobic surfaces show long-term stability over a wide pH range, that is, not only for pure water but also for corrosive liquids including acidic and basic solutions. We expect that this technique will make it possible for large-scale production of super-hydrophobic engineering materials with new industrial applications.

**ACKNOWLEDGEMENTS** This work was subsidized by the National Natural Science Foundation of China (50575218).

#### REFERENCES

- 1 H. Gau, S. Herminghaus, P. Lenz, R. Lipowsky, *Science* **283**, 46 (1999)
- 2 A. Nakajima, A. Fujishima, K. Hashimoto, T. Watanabe, *Adv. Mater.* **11**, 1365 (1999)
- 3 A. Nakajima, K. Hashimoto, T. Watanabe, *Monatsh. Chem.* **132**, 31 (2001)
- 4 P. Gould, *Mater. Today* **6**, 44 (2003)
- 5 T. Sun, L. Feng, X. Gao, L. Jiang, *Acc. Chem. Res.* **38**, 644 (2005)
- 6 F. Xia, L. Feng, S. Wang, T. Sun, W. Song, W. Jiang, L. Jiang, *Adv. Mater.* **18**, 432 (2006)
- 7 T. Sun, G. Wang, L. Feng, B. Liu, Y. Ma, L. Jiang, D. Zhu, *Angew. Chem. Int. Edit.* **43**, 357 (2004)
- 8 R. Blossey, *Nat. Mater.* **2**, 301 (2003)
- 9 W. Barthlott, C. Neinhuis, *Planta* **202**, 1 (1997)
- 10 C. Neinhuis, W. Barthlott, *Ann. Bot.* **79**, 667 (1997)
- 11 T. Wagner, C. Neinhuis, W. Barthlott, *Acta Zool.* **20**, 7665 (2004)
- 12 K.K.S. Lau, J. Bico, K.B.K. Teo, M. Chowalla, G.A.J. Amarantunga, W.I. Milne, G.H. McKinley, K.K. Gleason, *Nano Lett.* **3**, 1701 (2003)
- 13 L. Feng, S. Li, H. Li, J. Zhai, Y. Song, L. Jiang, D. Zhu, *Angew. Chem. Int. Edit.* **41**, 1221 (2002)
- 14 J.L. Zhang, J. Li, Y.C. Han, *Macromol. Rapid Commun.* **25**, 1105 (2004)
- 15 M.H. Jin, X.J. Feng, J.M. Xi, J. Zhai, K.W. Cho, L. Feng, L. Jiang, *Macromol. Rapid Commun.* **26**, 1805 (2005)
- 16 H.Y. Erbil, A.L. Demirel, Y. Avci, O. Mert, *Science* **299**, 1377 (2003)
- 17 Q.D. Xie, J. Xu, L. Feng, L. Jiang, W.H. Tang, X.D. Luo, C.C. Han, *Adv. Mater.* **16**, 302 (2004)
- 18 X.J. Zhang, J. Tian, L.J. Wang, Z.F. Zhou, *J. Petrol. Sci. Eng.* **36**, 87 (2002)
- 19 J. Tian, Z.F. Zhou, CN Pat, ZL95104124.X (1999)
- 20 A.B.D. Cassie, S. Baxter, *Trans. Faraday Soc.* **40**, 546 (1944)
- 21 D. Que'ré, *Nature Mater.* **1**, 14 (2002)